JACS
JOURNAL OF THE AMERICAN CHEMICAL SOCIETY
Article
pubs.acs.org/JACS

Valence Tautomerization of High-Valent Manganese(V)-Oxo Corrole Induced by Protonation of the Oxo Ligand

Curt J. Bougher,[†] Shuo Liu,[†] Scott D. Hicks,[†] and Mahdi M. Abu-Omar*[,†,‡]

[†]Brown Laboratory, Department of Chemistry, Negishi-Brown Institute for Catalysis (NBIC), Purdue University, 560 Oval Drive, West Lafayette, Indiana 47907, United States

[‡]School of Chemical Engineering, Purdue University, Forney Hall of Chemical Engineering, 480 Stadium Mall Drive, West Lafayette, Indiana 47907, United States

Supporting Information

ABSTRACT: The addition of an organic acid to the manganese(V)-oxo corrole complex (tpfc)$Mn^{V}(O)$ (tpfc = 5,10,15-tris(pentafluorophenyl)-corrole) induces valence tautomerization resulting in the formation of $(tpfc^{+\bullet})Mn^{IV}(OH)$ in acetonitrile at 298 K. The corrole radical cation manganese(IV) hydroxo complex has been fully characterized by EPR, ^{1}H NMR, and UV−vis spectroscopy. The reactivity of the valence tautomer $(tpfc^{+\bullet})Mn^{IV}(OH)$ is compared to that of (tpfc)$Mn^{V}(O)$ in three reaction types: hydrogen atom transfer (HAT), electron transfer (ET), and oxygen atom transfer (OAT). $(tpfc^{+\bullet})Mn^{IV}(OH)$ shows a dramatic 5 orders of magnitude enhancement in the rate of ET but surprisingly does not undergo OAT with PhSMe. The high-valent (tpfc)$Mn^{V}(O)$ complex is moderately more reactive toward HAT with substituted phenol and shows superior activity in OAT.

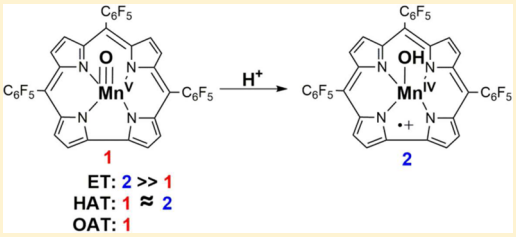

INTRODUCTION

High-valent metal−oxo complexes are important in biological transformations and oxidation reactions.[1−11] Proper deduction of their reactivity is an essential step in understanding heme enzymes and bioinspired synthetic heme-type catalysts.[12] For example, the hydroxylation of C−H bonds in cyctochrome P450 has been thought to proceed via one of two reactive intermediates, $Fe^{V}(O)$ $(Por^{+\bullet})$ (Compound I) or $Fe^{IV}(O)$ (Por) (Compound II), and until recently[13] was a matter of much debate.[6,14−20] Studies of synthetic high-valent iron and manganese heme-type complexes have contributed significantly to establishing the mechanism of P450 and the general understanding of high-valent heme chemistry.[21] High-valent Mn-oxo species have been proposed as key intermediates in a large range of synthetic heme and nonheme Mn-catalyzed oxidation reactions[22,23] as well as water oxidation in photosystem II.[24,25]

We report herein an example of a manganese-oxo porphyrinoid valence tautomer complex using a Brønsted acid. The reaction of manganese(V)-oxo corrole ((tpfc)-$Mn^{V}(O)$, tpfc = tris(pentafluorophenyl)corrole) with trifluoroacetic acid (TFA) in acetonitrile forms the manganese(IV)-hydroxo cation radical corrole complex $(tpfc^{+\bullet})Mn^{IV}(OH)$ as shown in Scheme 1. Both species have been fully characterized, providing insight into the reactivity of high-valent manganese-(V) oxo and manganese(IV) hydroxo cation radical compounds. This work was compared to the valence tautomerization of manganese-oxo corrolazine $(TBP_8Cz)Mn^{V}(O)$ [TBP_8Cz = octakis(*p-tert*-butylphenyl)corrolazinato)$^{3-}$] with Lewis and Brønsted acids (LA = Zn^{2+}, $B(C_6F_5)$, or H^{+}) to form the cation radical corrolazine $(TBP_8Cz^{+\bullet})Mn^{IV}$(O-LA) published by Goldberg et al.[26−28] The complexes $(tpfc^{+\bullet})$-$Mn^{IV}(OH)$ and (tpfc)$Mn^{V}(O)$ undergo hydrogen atom-transfer (HAT) and electron-transfer (ET) reactions. Rates of HAT, ET, and oxygen atom-transfer (OAT) were experimentally determined highlighting the stark difference in reactivity of (tpfc)$Mn^{V}(O)$ versus $(tpfc^{+\bullet})Mn^{IV}(OH)$ species.

Scheme 1

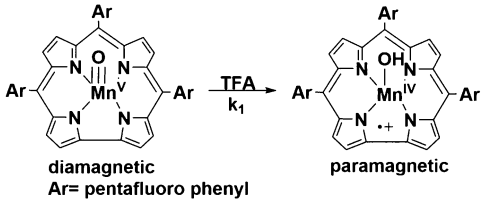

EXPERIMENTAL SECTION

Chemicals and Reagents. All reactions were carried out in acetonitrile CROMASOLV Plus with HPLC ≥ 99.9% purity obtained from Sigma-Aldrich. Alumina was activated overnight under vacuum with heating. Pyrrole and pentafluorobenzaldehyde were obtained from Sigma-Aldrich and distilled prior to use. Iodosobenzene was obtained from TCI. Trifluoroacetic acid was obtained from Sigma-Aldrich. Dry and degassed solvents were obtained from a Pure Processing Technology (PPT) solvent purification system. UV−vis spectra and kinetics were recorded on a Cary-60 spectrophotometer equipped with a temperature controller capable of holding four cells. Kinetic measurements with short half-lifetimes (<10 s) were

Received: September 16, 2015
Published: October 30, 2015

DOI: 10.1021/jacs.5b09759
J. Am. Chem. Soc. 2015, 137, 14481−14487

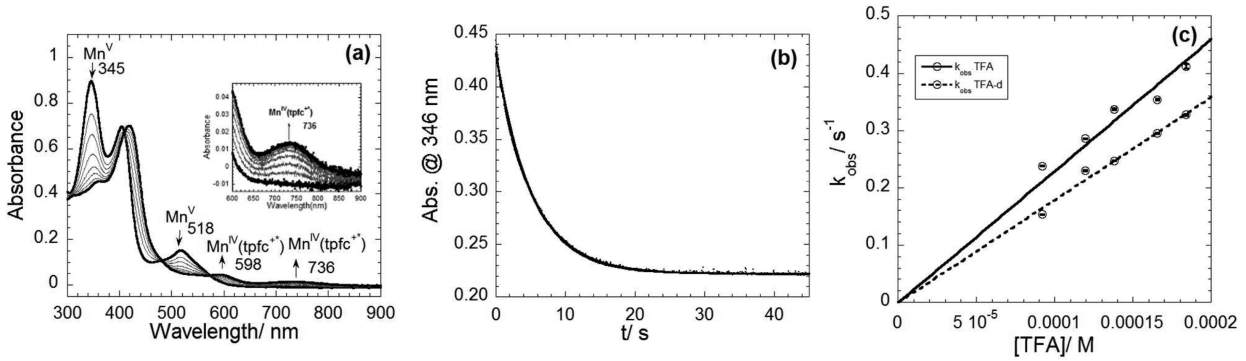

Figure 1. Plots corresponding to the formation of $(tpfc^{+\bullet})Mn^{IV}(OH)$ (a) UV−vis spectral changes for the reaction of $(tpfc)Mn^{V}(O)$ with TFA (20 equiv) at 25 °C. (b) Absorbance change at 346 nm versus time corresponding to the formation of $(tpfc^{+\bullet})Mn^{IV}(OH)$ (points) and best fit (solid line). (c) KIE in the reaction of $(tpfc)Mn^{V}(O)$ with TFA and TFA-d with k_H = 2300 ± 70 M^{-1} s^{-1}, k_D = 1800 ± 25 M^{-1} s^{-1}, and k_H/k_D = 1.28 ± 0.04.

performed on an Applied Photophysics stopped-flow spectrophotometer with monochromator attachment for single wavelength kinetics. NMR spectra were obtained on Bruker 500 MHz spectrometers. The compounds H_3(tpfc) and Mn(tpfc) were prepared according to modified literature procedures.[29−31]

Synthesis of H_3(tpfc).[29,31] H_3(tpfc) was prepared by modified literature methods conducted under a nitrogen atmosphere unless otherwise specified. In a 250 mL round-bottom flask, activated basic alumina (14.0 g) was covered with minimal dichloromethane followed by the addition of pyrrole (5.09 g, 75.9 mmol) and pentafluorobenzaldehyde (14.7 g, 75.9 mmol). The mixture was then allowed to stir and was heated to 60 °C open to the atmosphere until a color change from yellow to brown was observed. The reaction mixture was then dissolved in 100 mL of dichloromethane and filtered to remove the alumina. 2,3-Dichloro-5,6-dicyano-1,4-benzoquinone (DDQ) was then added to the reaction mixture over 30 min to afford a color change from brown to black over 8 h. The mixture was filtered to remove any unreacted DDQ. The solution was purified by column chromatography using basic alumina and dichloromethane:hexanes (1:1) as the eluent. The red fluorescent fraction was monitored by UV light, collected, and concentrated under reduced pressure resulting in a deep colored solid. This solid was further purified on a separate column using basic alumina with dichloromethane:hexanes as the eluent starting at 1:2 and slowly changing to 2:1. The solvent was removed with rotary evaporation and recrystallized from dichloromethane and hexanes, giving a 5% yield (0.95 mmol.)

Synthesis of $(tpfc)Mn^{III}$.[29−32] According to a modified literature procedure, $(tpfc)Mn^{III}$ was prepared by refluxing H_3(tpfc) (300 mg, 0.36 mmol) and $Mn^{II}(OAc)_2{\cdot}4H_2O$ (923 mg, 3.6 mmol) in 50 mL of dry DMF for 20 min open to the atmosphere. The solvent was removed by rotary evaporation resulting in a green solid. The solid was purified by column chromatography using silica with ethyl acetate:hexanes as the eluent in a 1:10 ratio and then changed to 3:10 ratio to force the green fraction off the column. The solvent was removed resulting in a solid that was recrystallized from ethyl acetate/heptane. UV−vis (MeCN): λ_{max} [nm] (log ε) = 401 (4.62), 419 (4.63), 595 (4.04), 615 (4.04). EPR data [g] parallel mode; acetonitrile:toluene (1:1) 5K 7.98.

Synthesis of $Mn^{V}(O)$ (tpfc).[30,32] $Mn^{V}(O)$ (tpfc) was prepared according to modified literature methods and found to be stable at all concentrations when kept air and moisture free. Mn^{III}(tpfc) (5 mg, 5 × 10^{-3} mmol) was dissolved in 5 mL of acetonitrile, and iodosobenzene (11 mg, 0.05 mmol) was mixed into the solution resulting in a color change from green to pink/orange. This mixture was than filtered to remove unreacted iodosobenzene. UV−vis (MeCN): λ_{max} [nm] (log ε) = 345 (4.65), 403 (4.54), 515 (3.95). ^{1}H NMR δ ($CDCl_3$): 9.50 (d, J = 5.0 Hz, 2 H), 9.18 (d, J = 5.0 Hz, 2 H), 8.99 (d, J = 5.0 Hz, 2 H), 8.93 (d, J = 5.0 Hz, 2 H).

Synthesis of $(tpfc^{+\bullet})Mn^{IV}(OH)$. $Mn^{IV}(OH)$ was prepared in situ by reacting 20 μM $Mn^{V}(O)$ (tpfc) with 1 equiv TFA in acetonitrile (Figure 1), resulting in a color change from pink/orange to yellow. The resulting species appeared to be more stable than the starting $Mn^{V}(O)$ (tpfc) with no decomposition on a time scale of days open to air and moisture. UV−vis (MeCN): λ_{max} [nm] (log ε) = 417 (4.56), 598 (3.62), 736 (3.28). EPR [g] perpendicular mode; acetonitrile:toluene (1:1) at 5 K: 5.85, 3.96, 2.00.

Spectroscopic and Kinetic Measurements. The tautomerization of $(tpfc)Mn^{V}(O)$ with TFA to $(tpfc^{+\bullet})Mn^{IV}(OH)$ in MeCN at 298 K was examined using UV−vis spectroscopy. The rate of the reaction was determined by the disappearance of the main soret for $(tpfc)Mn^{V}(O)$ at 345 nm. Electron transfer from dimethyl ferrocene (Me_2Fc) to $(tpfc)Mn^{V}(O)$ in MeCN at 270 K was monitored using a Applied Photophysics SX.18MV stopped-flow. HAT from 2,4-ditertbutyl phenol (2,4-DTBP) to $(tpfc)Mn^{V}(O)$ in MeCN at 298 K was monitored using Agilent Cary 60 UV−vis spectroscopy. HAT rate constants of $(tpfc)Mn^{V}(O)$ and $(tpfc^{+\bullet})Mn^{IV}(OH)$ forming the corresponding $(tpfc)Mn^{III}(OH_2)$ using 2,4-ditertbutylphenol were determined from single wavelength measurements on the Cary 60 UV−vis spectrophotometer.

EPR Measurements. Samples were prepared in a glovebox with a mixture of 50:50 toluene acetonitrile. All samples were prepared from a 0.5 mM stock solution of $(tpfc)Mn^{III}$ with an addition of 1 equiv of reagent. After removal from the glovebox, the sample was frozen in liquid nitrogen. EPR measurements were performed using a Bruker X-band EPR spectrometer equipped with a dual mode cavity (ER 4116DM) in perpendicular and parallel mode. Oxford Instruments ESR900 liquid HE quartz cryostat with an Oxford Instruments ITC503 temperature and gas flow controller was used to achieve and control low temperature. The experimental parameters for perpendicular mode EPR spectra were as follows: Microwave frequency = 9.65 GHz, microwave power = 31.7 mW, modulation amplitude = 10 G, gain = 1 × 10^4, modulation frequency = 100 kHz, time constant = 20.48 ms, and conversion time = 30 ms. Parameters for parallel mode EPR spectra were the same except Microwave frequency = 9.39 GHz. The EPR spectra were measured under nonsaturating microwave power conditions. The amplitude of modulation was chosen to optimize the resolution and the signal-to-noise (S/N) ratio of the observed spectra.

RESULTS AND DISCUSSION

Synthesis and Characterization of Manganese(IV) Hydroxo Corrole Cation Radical Complex. The synthetic route to the first well-characterized manganese(IV) hydroxo corrole cation radical complex is discussed. This complex was derived from the reaction of $(tpfc)Mn^{V}(O)$ with 1 equiv trifluoroacetic acid via protonation of the manganese(V)-oxo species, resulting in a gradual color change from red to yellow. Reaction kinetics were monitored by the decrease in absorbance at 346 and 518 nm, corresponding to the

DOI: 10.1021/jacs.5b09759
J. Am. Chem. Soc. 2015, 137, 14481−14487

disappearance of (tpfc)Mn^{V}(O) (Figure 1a). The absorbance band at 403 nm red shifts to 417 nm, and the absorbance bands at 598 and 736 nm increase representing the formation of (tpfc$^{+\bullet}$)Mn^{IV}(OH). The addition of excess acid (1−20 equiv) led to no further change of (tpfc$^{+\bullet}$)Mn^{IV}(OH) according to UV−vis spectra. A decrease in the molar absorptivity of the soret band at 417 nm and the appearance of a weaker, broad, long-wavelength band at 736 nm are characteristic of π-cation radical in porphyrins and corroles.[33,34] The pseudo-first-order rate constants (k_{obs}) were plotted versus [TFA] giving a second-order rate k_1 = 2300 ± 70 M^{-1} s^{-1}. To further prove proton transfer, deuterated TFA was used with a kinetic isotope effect (KIE) of 1.3 was observed (Figure 1c).

To validate the formation of (tpfc$^{+\bullet}$)Mn^{IV}(OH), EPR spectroscopy measurements were acquired as shown in Figure 2. The EPR spectrum obtained agrees with a Mn^{IV} (S = 3/2)

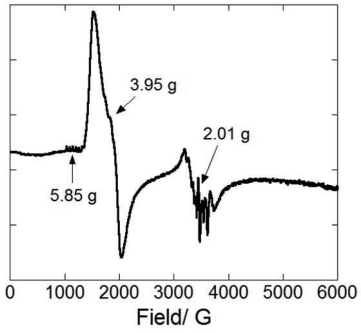

Figure 2. EPR spectrum of (tpfc$^{+\bullet}$)Mn^{IV}(OH), peak at g = 5.85 has 6 line hyperfine indicative of a monomeric manganese species, g = 3.95 is expected for a Mn^{IV} S = 3/2, and 9 line hyperfine at g = 2.01 indicates a free radical on the corrole split by the 4 ligand nitrogens.

species with an uncoupled cation radical peak with hyperfine splitting of the corrole nitrogens.[12,21,22,35,36] The signal at g = 5.85 shows a 6 line hyperfine splitting, which is indicative of a monomeric manganese species.[37] The signals observed at g = 5.85 and 3.95 are consistent with a S = 3/2, which is expected for a Mn^{IV} species.[38] The peak at g = 2.01 shows a 9 line hyperfine splitting that is consistent with a free radical on corrole split by the 4 corrole nitrogens. These data are consistent with what is expected for (tpfc$^{+\bullet}$)Mn^{IV}(OH).

Kinetic studies of ET Reactions with Manganese-Oxo Corrole. The reaction kinetics for ET of (tpfc)Mn^{V}(O) using dimethyl ferrocene (Me_2Fc) were measured. Upon the addition of ≥1 equiv of Me_2Fc to (tpfc)Mn^{V}(O), the Mn^{V}(O) is reduced to [(tpfc)Mn^{IV}(O)]$^{-}$, as shown in Figure 3. The absorption bands at 468 and 610 nm increase (Figure 3a) and are assigned to the appearance of [(tpfc)Mn^{IV}(O)]$^{-}$. The evident and clean isosbestic points are indicative of no accumulation of an intermediate. This change was accompanied by a decrease in the absorbance band at 346 nm signifying the disappearance of (tpfc)Mn^{V}(O). Reaction kinetics of the reduction of Mn^{V}(O) to [Mn^{IV}(O)]$^{-}$ were monitored on a stopped flow at −4 °C by following the absorbance increase at 468 nm with excess Me_2Fc. Pseudo-first-order rate constants (k_{obs}) were plotted versus [Me_2Fc] giving a second-order rate constant of 2.2 × 10^5 M^{-1} s^{-1}, Figure 3c.

The starting (tpfc)Mn^{V}(O) species is diamagnetic, gives a characteristic NMR spectrum (Figure S4), and is EPR silent, which is expected for a low-spin d^2 manganese(V) species.[30,32] Upon reaction of the Mn^{V}(O) with Me_2Fc, an EPR signal

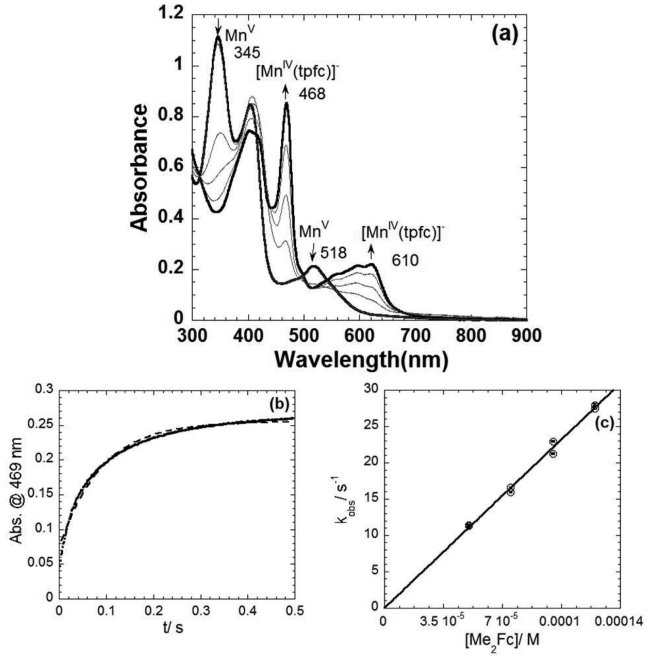

Figure 3. Plots corresponding to ET of (tpfc)Mn^{V}(O) with Me_2Fc (a) Time-resolved UV−vis spectra of (tpfc)Mn^{V}(O) + Me_2Fc (1 equiv) at −4 °C. (b) Kinetic trace at 469 nm versus time corresponding to the formation of (tpfc)Mn^{IV} (dots) and best fit (dashed line). (c) Plot of k_{obs} versus [Me_2Fc] with the slope being the second-order rate constant of ET (k_2) = 220,000 ± 2100 M^{-1} s^{-1}.

corresponding to a Mn^{IV} (S = 3/2) was observed, Figure 4, and the NMR signal from the corrole disappeared, confirming that

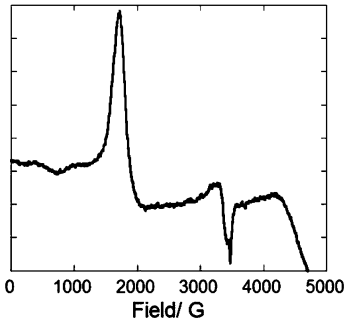

Figure 4. EPR spectra of [(tpfc)Mn^{IV}(O)]$^{-}$ (S = 1/2) at 5 K, formed from the reaction of (tpfc)Mn^{V}(O) and Me_2Fc.

the [(tpfc)Mn^{IV}(O)]$^{-}$ species was formed. Therefore, on the basis of UV−vis, NMR, and EPR spectroscopy we conclude that the product from the reaction of (tpfc)Mn^{V}(O) with Me_2Fc is [(tpfc)Mn^{IV}(O)]$^{-}$, Scheme 2. In the case of Goldberg's (TBP_8Cz)Mn^{V}(O) species, a two-electron reduction to form the (TBP_8Cz)Mn^{III} was observed with no observable Mn^{IV}.[26] However, with our complex the two-electron reduction is not observed but rather a one-electron reduction to form [(tpfc)Mn^{IV}(O)]$^{-}$. Another difference is the

Scheme 2

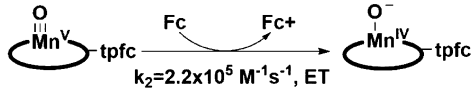

DOI: 10.1021/jacs.5b09759
J. Am. Chem. Soc. 2015, 137, 14481−14487

requirement of more strongly reducing ferrocene derivatives for Goldberg's Mn-oxo corrolazine, whereas our (tpfc)Mn^{V}(O) can be reduced with ferrocene.[26] The (TBP_8Cz)Mn^{V}(O) has an ET second-order rate constant of 7.5×10^4 M^{-1} s^{-1} with octamethyl ferrocene,[26] whereas the (tpfc)Mn^{V}(O) in this study has an ET second-order rate constant of 2.2×10^5 M^{-1} s^{-1} with dimethyl ferrocene.

Kinetic Studies of ET Reactions with Manganese(IV)-Hydroxo Cation Radical Corrole. The ET reaction kinetics of (tpfc$^{+\bullet}$)Mn^{IV}(OH) using dimethyl ferrocene (Me_2Fc) were investigated. Upon the addition of Me_2Fc, (tpfc$^{+\bullet}$)Mn^{IV}(OH) is reduced all the way to (tpfc)Mn^{III}, Scheme 3. The reaction was

Scheme 3

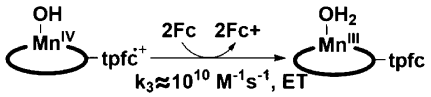

monitored by the appearance of an absorbance band at 600 nm using stopped flow UV−vis spectroscopy at −4 °C. The latter band is assigned to (tpfc)Mn^{III}, as reported previously.[29−32] The pseudo-first-order rate constants (k_{obs}) were too fast to be determined by stopped flow surmising a second-order rate constant $\geq 10^7$ M^{-1} s^{-1}.

To determine the rate constant, Marcus theory was applied to this system. The rate constant for the intermolecular ET rate constant (k_{ET}) was evaluated using the Marcus cross relationship (eq 1):

$$k_{ET} = (k_{11}k_{22}K_{12}f)^{1/2} \quad (1)$$

k_{11} and k_{22} are the rate constants for self-exchange reactions, K_{12} is the ET equilibrium constant, and f is a frequency factor close to unity.[39] According to the Marcus cross relationship (eq 1), the rate constant of intermolecular ET was estimated to be in the range of 3×10^9−3×10^{10} M^{-1} s^{-1} using k_{11} of 5.3×10^6 M^{-1} s^{-1} for Me_2Fc/Me_2Fc^+,[40] k_{22} value of 1×10^9−1×10^{11} M^{-1} s^{-1} [41,42] based on values for porphyrin species, and a K_{12} value (calculated from $E_{1/2}$ of the cyclic voltammetry of (tpfc$^{+\bullet}$)Mn^{IV}(OH), Figure S2) of 1.9×10^3. The estimated rate constant is consistent with the experimental measurements that $k_{ET} > 10^7$ M^{-1} s^{-1}. In comparing to the corrolazine system, ($TBP_8Cz^{+\bullet}$)Mn^{IV}(O-Zn^{2+}) reacts with ferrocene to give the characteristic spectrum for Mn^{IV} and closed-shell corrolazine ligand.[26] This difference in reactivity between corrole and corrolazine underscores how differences in the ligand affect the outcome of ET reactions.

Cation Radical/Hydroxo Effect on ET. The ET rates of (tpfc)Mn^{V}(O) and (tpfc$^{+\bullet}$)Mn^{IV}(OH) vary greatly. The ET rate constant for (tpfc)Mn^{V}(O) was measured to be 2.2×10^5 M^{-1} s^{-1}, whereas the ET rate for (tpfc$^{+\bullet}$)Mn^{IV}(OH) was faster than can be determined by stopped-flow. The ET rate constant for (tpfc$^{+\bullet}$)Mn^{IV}(OH) was calculated to be approximately 10^9−10^{10} M^{-1} s^{-1} using the Marcus theory. These results parallel those observed by Goldberg for corrolazine, where the cation radical is reduced by ferrocene, whereas the Mn^{V}(O) corrolazine required the more strongly reducing Me_8Fc.[26] Both complexes (tpfc)Mn^{V}(O) and (tpfc$^{+\bullet}$)Mn^{IV}(OH) in our study herein undergo ET with ferrocene, but the difference in rate between the two shows that (tpfc$^{+\bullet}$)Mn^{IV}(OH) is more reactive in ET by 5 orders of magnitude (x 10^5). Although both the corrole and corrolazine show the radical cation to be more reactive in ET, there are significant differences. In the case of ET to (tpfc)Mn^{V}(O), a one-electron reduction occurs resulting in a stable [Mn^{IV}-oxo]$^-$ corrole, whereas (TBP_8Cz)Mn^{V}(O) undergoes a two-electron reduction forming Mn^{III} corrolazine with no observable Mn^{IV} intermediate.[26] Similarly, the (tpfc$^{+\bullet}$)Mn^{IV}(OH) undergoes a two-electron reduction to form (tpfc)Mn^{III}, whereas ($TBP_8Cz^{+\bullet}$)Mn^{IV}(O−Zn) undergoes a one-electron reduction to form [(TBP_8Cz)Mn^{IV}(O−Zn)]$^+$.[26]

Kinetic Studies of HAT Reactions with Manganese-Oxo Corrole. HAT reaction kinetics of (tpfc)Mn^{V}(O) using 2,4-$(tBu)_2$ phenol were measured. The absorption bands at 346 and 518 nm decreased with clean isosbestic points (Figure 5a).

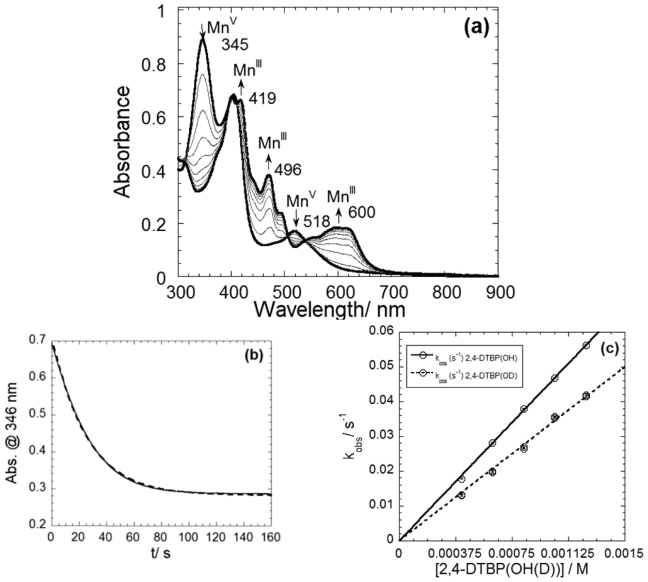

Figure 5. Plots corresponding to HAT of (tpfc)Mn^{V}(O) with 2,4-DTBP (a) Time-resolved UV−vis spectra of (tpfc)Mn^{V}(O) + 2,4-DTBP (20 equiv) at 25 °C. (b) Change in absorbance at 346 nm versus time corresponding to the formation of (tpfc)Mn^{III} (dots) and best fit (dashed line). (c) KIE in the reaction of (tpfc)Mn^{V}(O) with 2,4-DTBP(OH) and 2,4-DTBP(OD) with $k_H = 45.0 \pm 0.3$ M^{-1} s^{-1}, $k_D = 33.7 \pm 0.3$ M^{-1} s^{-1}, and $k_H/k_D = 1.34 \pm 0.02$.

This change was accompanied by an increase in absorbance bands at 401, 496, and 600 nm that are assigned to (tpfc)Mn^{III}.[30,31] Reaction kinetics for the reduction of (tpfc)-Mn^{V}(O) to (tpfc)Mn^{III} were monitored by the decrease in absorbance at 346 nm. Pseudo-first-order rate constants (k_{obs}) were plotted versus [2,4-DTBP] giving a second-order rate constant of 45 M^{-1} s^{-1} (Figure 5b). The KIE was measured using 2,4-DTBP(OD), resulting in a KIE of 1.3 (Figure 5c).

The starting (tpfc)Mn^{V}(O) species is diamagnetic and gives a characteristic NMR spectrum.[31] An EPR signal corresponding to a Mn(III) ($S = 2$)[43] was observed in the EPR in parallel mode upon the reaction of Mn^{V}-oxo with 2,4-ditertbutylphenol (Figure S5).[22,44−46] Therefore, on the basis of UV−vis, NMR, and EPR spectroscopy we conclude that the product from the reaction of (tpfc)Mn^{V}(O) with 2,4-ditertbutylphenol is a manganese(III)-H_2O adduct, Scheme 4.

Kinetic Studies of HAT Reactions with Manganese(IV)-Hydroxo Cation Radical Corrole. The HAT reaction kinetics of (tpfc$^{+\bullet}$)Mn^{IV}(OH) using 2,4-ditertbutylphenol were investigated. The reaction was monitored following an increase in the absorption bands at 496 nm with clean isosbestic points. The latter band is assigned to (tpfc)Mn^{III}, as reported previously.[29−31] The kinetics of the reduction of

DOI: 10.1021/jacs.5b09759
J. Am. Chem. Soc. 2015, 137, 14481−14487

Scheme 4

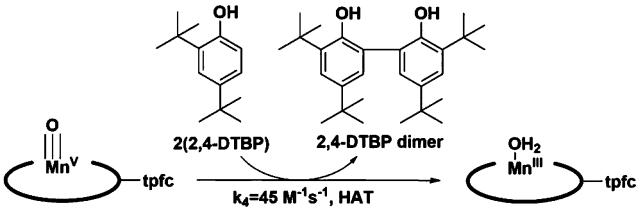

$(tpfc^{+\bullet})Mn^{IV}(OH)$ to $(tpfc)Mn^{III}$ were investigated following the increase in absorbance at 496 nm. Pseudo-first-order rate constants (k_{obs}) were plotted versus [2,4-DTBP] giving a second-order rate constant of 33 M^{-1} s^{-1} (Figure 6b.) The KIE

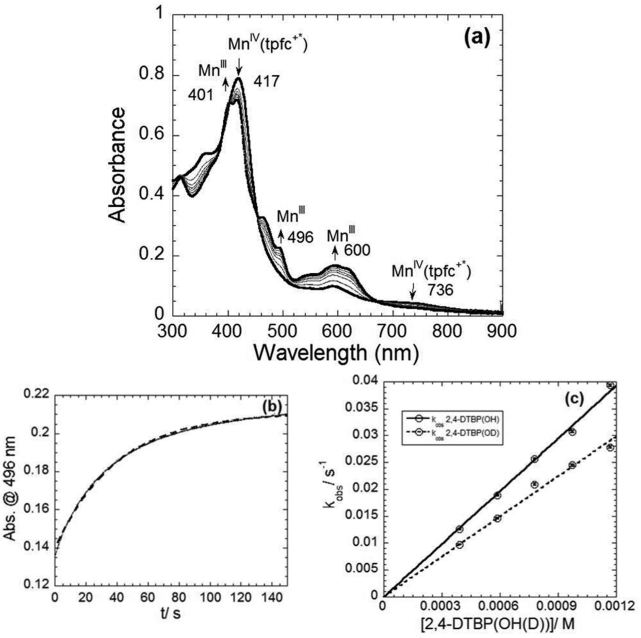

Figure 6. Plots corresponding to HAT of $(tpfc^{+\bullet})Mn^{IV}(OH)$ with 2,4-DTBP (a) Time-resolved UV−vis spectra of $(tpfc^{+\bullet})Mn^{IV}(OH)$ + 2,4-DTBP(20 equiv) at 25 °C. (b) Change in absorbance at 496 nm versus time corresponding to the formation of $(tpfc)Mn^{III}$ (dots) and best fit (dashed line). (c) KIE in the reaction of $(tpfc^{+\bullet})Mn^{IV}(OH)$ with 2,4-DTBP(OH) and 2,4-DTBP(OD) with k_H = 32.6 ± 0.4 M^{-1} s^{-1}, k_D = 25.2 ± 0.5 M^{-1} s^{-1}, and k_H/k_D = 1.3 ± 0.03.

was measured using 2,4-DTBP(OD) resulting in a KIE of 1.3 (Figure 6c). The presence of a KIE confirms that the rate is dependent on the HAT step of the reaction (Scheme 5). This observation leads to the conclusion that the HAT is the rate limiting step of the reaction.

The absorption bands at 417, 598, and 736 nm (π-cation radical in porphyrinoid species)[26,33,34] associated with $(tpfc^{+\bullet})$-$Mn^{IV}(OH)$ change gradually (Figure 6a). These spectral changes were accompanied by an increase in absorbance bands at 401, 496, and 600 nm assigned to $(tpfc)Mn^{III}$.[29−31] Upon addition of 2,4-DTBP to $(tpfc^{\bullet+})Mn^{IV}(OH)$ there was no longer a perpendicular mode EPR signal, but a parallel mode spectrum corresponding to high-spin $(tpfc)Mn^{III}$ (S = 2)[22,43,46] was observed (Figure S5). Therefore, on the basis of UV−vis and EPR spectroscopy, we conclude that the product from the reaction of the Mn(IV) corrole cation radical complex with 2,4-ditertbutylphenol is a manganese(III)-H_2O adduct (Scheme 6), and per the experimental KIE, the rate-determining step is HAT as delineated in Scheme 5.

Scheme 6

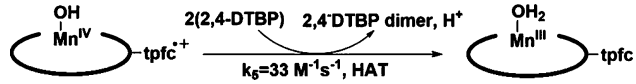

Cation Radical/Hydroxo Effect on HAT. The HAT rate of reaction with the manganese(V)-oxo corrole versus the manganese(IV)-hydroxo cation radical corrole vary but within a narrow range. The rate of HAT for $(tpfc)Mn^{V}(O)$ was determined to be 45 M^{-1} s^{-1}, whereas the rate of HAT for $(tpfc^{+\bullet})Mn^{IV}(OH)$ was determined to be 33 M^{-1} s^{-1}. KIE studies were done with both $(tpfc)Mn^{V}(O)$ and $(tpfc^{+\bullet})$-$Mn^{IV}(OH)$ giving a primary KIE for both of approximately 1.3 (Figures 5c and 6c). In contrast to ET reactions, it appears that the corrole valence tautomers do not exhibit different reactivity in HAT reactions.

The reaction of $(tpfc^{+\bullet})Mn^{IV}(OH)$ with 2,4-ditertbutylphenol to afford $(tpfc)Mn^{III}(OH_2)$ appears to follow a HAT step first followed by an ET (Scheme 5). The reaction of $(tpfc)Mn^{V}(O)$ with 2,4-ditertbutylphenol appears to proceed via HAT with 2 equiv of the 2,4-DTBP. Our results are in sharp contrast to Goldberg's, where HAT with Mn^{IV} corrolazine cation radical was faster than with $Mn^{V}(O)$ corrolazine.[26−28] Another difference observed with corrolazine is with the stability of the single HAT event to the tautomer resulting in a stable Mn^{IV},[26] whereas HAT with the corrole complex herein results in an unstable Mn^{IV} species leading to the formation of Mn^{III} as the final product. The UV−vis and EPR spectral features are consistent with the assigned oxidation states. The addition of excess 2,4-DTBP does not lead to any further spectral change of the manganese corrole complex.

Cation Radical/Hydroxo Effect on OAT. Oxygen atom transfer was studied for both $(tpfc)Mn^{V}(O)$ and $(tpfc^{+\bullet})$-$Mn^{IV}(OH)$ using thioanisole, PhSMe, as the oxygen acceptor. No OAT is observed for $(tpfc^{+\bullet})Mn^{IV}(OH)$ when reacted with PhSMe, whereas with $(tpfc)Mn^{V}(O)$ OAT to PhSMe was observed (Scheme S2). The product from the reaction of $(tpfc)Mn^{V}(O)$ with PhSMe is $(tpfc)Mn^{III}$ and sulfoxide, PhSOMe, as seen by UV−vis (Figure S6a) and EPR spectroscopy. The pseudo-first-order rate constant (k_{obs}) was

Scheme 5

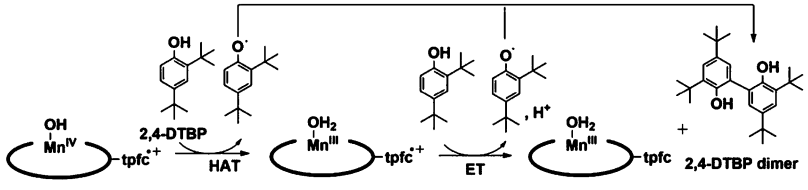

DOI: 10.1021/jacs.5b09759
J. Am. Chem. Soc. 2015, 137, 14481−14487

used to obtain a second-order rate constant for OAT of 0.70 M^{-1} s^{-1} (Figure S6b). Similarly, Goldberg reports that the Mn^{V}(O) corrolazine was more active in OAT than the valence tautomer Mn^{IV}(O-LA) cation radical corrolazine (LA = Zn^{2+}, $B(C_6F_5)_3$ H^+).[27]

CONCLUSION

Mn(IV)-hydroxo corrole radical cation has been prepared by the reaction of Mn(V)-oxo corrole with TFA. While the valence tautomer (tpfc$^{+\bullet}$)Mn^{IV}(OH) is more stable than (tpfc)Mn^{V}(O) (days versus hours in open air and moisture), it exhibits enhanced reactivity in ET reactions, a rate enhancement by approximately 5 orders of magnitude (Scheme 7). In HAT

Scheme 7

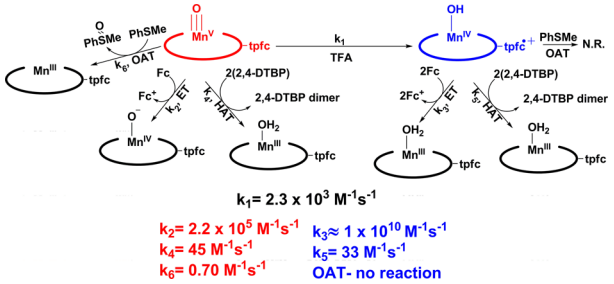

reactions with 2,4-$(tBu)_2$ phenol both valence tautomers exhibit comparable rate constants and identical KIE. While (tpfc)-Mn^{V}(O) is capable of undergoing OAT with PhSMe with a second-order rate constant of 0.70 M^{-1} s^{-1}, (tpfc$^{+\bullet}$)Mn^{IV}(OH) does not react at all with PhSMe (Scheme 7). These differences illustrate the importance of valence and electronic structure on redox reactions of high-valent porphyrinoid complexes.

ASSOCIATED CONTENT

Supporting Information

The Supporting Information is available free of charge on the ACS Publications website at DOI: 10.1021/jacs.5b09759.

UV−vis spectra, cyclic voltammetry, EPR, NMR, and kinetics for OAT (PDF)

AUTHOR INFORMATION

Corresponding Author

*mabuomar@purdue.edu

Notes

The authors declare no competing financial interest.

ACKNOWLEDGMENTS

This research was supported by a grant from the U.S. National Science Foundation (NSF grant no. CHE-1463900).

REFERENCES

(1) Czernuszewicz, R. S.; Mody, V.; Czader, A.; Gałęzowski, M.; Gryko, D. T. *J. Am. Chem. Soc.* **2009**, *131*, 14214.
(2) Ostovic, D.; Bruice, T. C. *Acc. Chem. Res.* **1992**, *25*, 314.
(3) Nam, W. *Acc. Chem. Res.* **2007**, *40*, 522.
(4) Shaik, S.; Hirao, H.; Kumar, D. *Acc. Chem. Res.* **2007**, *40*, 532.
(5) Franke, A.; Hessenauer-Ilicheva, N.; Meyer, D.; Stochel, G.; Woggon, W.-D.; van Eldik, R. *J. Am. Chem. Soc.* **2006**, *128*, 13611.
(6) Meunier, B.; de Visser, S. P.; Shaik, S. *Chem. Rev.* **2004**, *104*, 3947.
(7) Zhang, R.; Newcomb, M. *Acc. Chem. Res.* **2008**, *41*, 468.
(8) Coelho, P. S.; Brustad, E. M.; Kannan, A.; Arnold, F. H. *Science* **2013**, *339*, 307.
(9) Denisov, I. G.; Makris, T. M.; Sligar, S. G.; Schlichting, I. *Chem. Rev.* **2005**, *105*, 2253.
(10) Meunier, B.; Adam, W. *Metal-oxo and metal-peroxo species in catalytic oxidations*; Springer: Berlin; New York, 2000.
(11) Ortiz de Montellano, P. R. *Cytochrome P450: Structure, Mechanism, and Biochemistry*, 3rd ed.; Kluwer Academic/Plenum Publishers: New York, 2005.
(12) Taguchi, T.; Stone, K. L.; Gupta, R.; Kaiser-Lassalle, B.; Yano, J.; Hendrich, M. P.; Borovik, A. S. *Chem. Sci.* **2014**, *5*, 3064.
(13) Rittle, J.; Green, M. T. *Science* **2010**, *330*, 933.
(14) Ortiz de Montellano, P. R. *Chem. Rev.* **2010**, *110*, 932.
(15) Hersleth, H.-P.; Ryde, U.; Rydberg, P.; Görbitz, C. H.; Andersson, K. K. *J. Inorg. Biochem.* **2006**, *100*, 460.
(16) Behan, R. K.; Green, M. T. *J. Inorg. Biochem.* **2006**, *100*, 448.
(17) Andersson, L. A.; D, J. H. *Struct. Bonding (Berlin, Ger.)* **1990**, *64*, 1.
(18) Chance, B.; Powers, L.; Ching, Y.; Poulos, T.; Schonbaum, G. R.; Yamazaki, I.; Paul, K. G. *Arch. Biochem. Biophys.* **1984**, *235*, 596.
(19) Penner-Hahn, J. E.; Smith Eble, K.; McMurry, T. J.; Renner, M.; Balch, A. L.; Groves, J. T.; Dawson, J. H.; Hodgson, K. O. *J. Am. Chem. Soc.* **1986**, *108*, 7819.
(20) MacBeth, C. E.; Gupta, R.; Mitchell-Koch, K. R.; Young, V. G.; Lushington, G. H.; Thompson, W. H.; Hendrich, M. P.; Borovik, A. S. *J. Am. Chem. Soc.* **2004**, *126*, 2556.
(21) Gupta, R.; Taguchi, T.; Borovik, A. S.; Hendrich, M. P. *Inorg. Chem.* **2013**, *52*, 12568.
(22) Taguchi, T.; Gupta, R.; Lassalle-Kaiser, B.; Boyce, D. W.; Yachandra, V. K.; Tolman, W. B.; Yano, J.; Hendrich, M. P.; Borovik, A. S. *J. Am. Chem. Soc.* **2012**, *134*, 1996.
(23) Guo, M.; Dong, H.; Li, J.; Cheng, B.; Huang, Y.-q.; Feng, Y.-q.; Lei, A. *Nat. Commun.* **2012**, *3*, 1190.
(24) Cady, C. W.; Crabtree, R. H.; Brudvig, G. W. *Coord. Chem. Rev.* **2008**, *252*, 444.
(25) McEvoy, J. P.; Brudvig, G. W. *Chem. Rev.* **2006**, *106*, 4455.
(26) Leeladee, P.; Baglia, R. A.; Prokop, K. A.; Latifi, R.; de Visser, S. P.; Goldberg, D. P. *J. Am. Chem. Soc.* **2012**, *134*, 10397.
(27) Zaragoza, J. P. T.; Baglia, R. A.; Siegler, M. A.; Goldberg, D. P. *J. Am. Chem. Soc.* **2015**, *137*, 6531.
(28) Baglia, R. A.; Prokop-Prigge, K. A.; Neu, H. M.; Siegler, M. A.; Goldberg, D. P. *J. Am. Chem. Soc.* **2015**, *137*, 10874.
(29) Gross, Z.; Galili, N.; Simkhovich, L.; Saltsman, I.; Botoshansky, M.; Bläser, D.; Boese, R.; Goldberg, I. *Org. Lett.* **1999**, *1*, 599.
(30) Gross, Z.; Golubkov, G.; Simkhovich, L. *Angew. Chem., Int. Ed.* **2000**, *39*, 4045.
(31) Zdilla, M. J.; Abu-Omar, M. M. *J. Am. Chem. Soc.* **2006**, *128*, 16971.
(32) Liu, H.-Y.; Lai, T.-S.; Yeung, L.-L.; Chang, C. K. *Org. Lett.* **2003**, *5*, 617.
(33) Simkhovich, L.; Mahammed, A.; Goldberg, I.; Gross, Z. *Chem. - Eur. J.* **2001**, *7*, 1041.
(34) Meier-Callahan, A. E.; Di Bilio, A. J.; Simkhovich, L.; Mahammed, A.; Goldberg, I.; Gray, H. B.; Gross, Z. *Inorg. Chem.* **2001**, *40*, 6788.
(35) Wang, C.; Kurahashi, T.; Inomata, K.; Hada, M.; Fujii, H. *Inorg. Chem.* **2013**, *52*, 9557.
(36) Yin, G.; McCormick, J. M.; Buchalova, M.; Danby, A. M.; Rodgers, K.; Day, V. W.; Smith, K.; Perkins, C. M.; Kitko, D.; Carter, J. D.; Scheper, W. M.; Busch, D. H. *Inorg. Chem.* **2006**, *45*, 8052.
(37) Taguchi, T.; Gupta, R.; Lassalle-Kaiser, B.; Boyce, D. W.; Yachandra, V. K.; Tolman, W. B.; Yano, J.; Hendrich, M. P.; Borovik, A. S. *J. Am. Chem. Soc.* **2012**, *134*, 1996.
(38) Parsell, T. H.; Behan, R. K.; Green, M. T.; Hendrich, M. P.; Borovik, A. S. *J. Am. Chem. Soc.* **2006**, *128*, 8728.
(39) Fukuzumi, S.; Mochizuki, S.; Tanaka, T. *Inorg. Chem.* **1989**, *28*, 2459.
(40) Yang, E. S.; Chan, M.-S.; Wahl, A. C. *J. Phys. Chem.* **1980**, *84*, 3094.

DOI: 10.1021/jacs.5b09759
J. Am. Chem. Soc. 2015, 137, 14481−14487

(41) Fukuzumi, S.; Endo, Y.; Imahori, H. *J. Am. Chem. Soc.* **2002**, *124*, 10974.
(42) Inamo, M.; Kumagai, H.; Harada, U.; Itoh, S.; Iwatsuki, S.; Ishihara, K.; Takagi, H. D. *Dalton Trans.* **2004**, 1703.
(43) Hendrich, M. P.; Debrunner, P. G. *Biophys. J.* **1989**, *56*, 489.
(44) Campbell, K. A.; Yikilmaz, E.; Grant, C. V.; Gregor, W.; Miller, A.-F.; Britt, R. D. *J. Am. Chem. Soc.* **1999**, *121*, 4714.
(45) Gonzalez-Riopedre, G.; Fernandez-Garcia, M. I.; Gonzalez-Noya, A. M.; Vazquez-Fernandez, M. A.; Bermejo, M. R.; Maneiro, M. *Phys. Chem. Chem. Phys.* **2011**, *13*, 18069.
(46) Krzystek, J.; Telser, J.; Pardi, L. A.; Goldberg, D. P.; Hoffman, B. M.; Brunel, L.-C. *Inorg. Chem.* **1999**, *38*, 6121.

DOI: 10.1021/jacs.5b09759
J. Am. Chem. Soc. 2015, 137, 14481−14487